



HAL
open science

Experimental investigation on a complex roof incorporating phase change material

Stéphane Guichard, Frédéric Miranville, Dimitri Bigot, Bruno Malet-Damour,
Harry Boyer

► **To cite this version:**

Stéphane Guichard, Frédéric Miranville, Dimitri Bigot, Bruno Malet-Damour, Harry Boyer. Experimental investigation on a complex roof incorporating phase change material. *Energy and Buildings*, 2015, 108, pp.36-43. 10.1016/j.enbuild.2015.08.055 . hal-01247436

HAL Id: hal-01247436

<https://hal.science/hal-01247436>

Submitted on 22 Dec 2015

HAL is a multi-disciplinary open access archive for the deposit and dissemination of scientific research documents, whether they are published or not. The documents may come from teaching and research institutions in France or abroad, or from public or private research centers.

L'archive ouverte pluridisciplinaire **HAL**, est destinée au dépôt et à la diffusion de documents scientifiques de niveau recherche, publiés ou non, émanant des établissements d'enseignement et de recherche français ou étrangers, des laboratoires publics ou privés.

1
2
3
4
5
6
7
8
9
10
11
12
13
14
15
16
17
18
19
20



Submission of manuscript to Energy and Buildings

Experimental investigation on a complex roof incorporating phase-change material.

Stéphane GUICHARD, Frédéric MIRANVILLE, Dimitri BIGOT, Bruno MALET-DAMOUR and Harry BOYER

Contents:

- *Manuscript*

Corresponding author:

Stéphane GUICHARD

Research Institute in Innovation and Business Sciences (IRISE) Laboratory\CESI-CCIR\CRITT

The CESI engineering school

Campus Pro - CCIR

65 rue du Père Lafosse - Boîte n°4

97410 Saint-Pierre

tél : 06 92 78 06 71

email : sguichard@cesi.fr



45		
46	<i>Nomenclature</i>	4
47	1. <i>Introduction</i>	5
48	2. <i>Research statement and methodology</i>	6
49	2.1. <i>Introduction</i>	6
50	2.2. <i>Research statement</i>	7
51	2.3. <i>Methodology</i>	8
52	3. <i>Experimental environment</i>	10
53	3.1. <i>The experimental platform</i>	10
54	3.2. <i>LGI test cell design</i>	11
55	3.3. <i>LGI test cell instrumentation</i>	12
56	3.4. <i>Description of PCM test</i>	13
57	3.5. <i>Climatic data and experimental sequences</i>	13
58	4. <i>Results</i>	14
59	4.1. <i>Introduction</i>	14
60	4.2. <i>Experimental results</i>	14
61	4.3. <i>Determination of the R-value</i>	16
62	5. <i>Conclusion</i>	17
63	6. <i>References</i>	19
64		
65		

66
67
68
69
70
71
72
73
74
75
76
77
78
79
80
81
82
83
84
85
86
87
88
89

Nomenclature

Variables

R Thermal resistance

T Temperature

Subscripts

i Interior

si Interior surface temperature

se Exterior surface temperature

Greek symbols

φ Heat flux

Abbreviations

ISOLAB A building simulation software, which integrates the hygro-thermal and
aeraulic phenomena

PCM Phase Change Material

RTAA DOM Thermal, Acoustic and Ventilation standards regulations in French overseas
department

90 1. Introduction

91 To combat global warming, it is necessary to reduce both energy consumption and the
92 emission of greenhouse gases. According to reference [1], energy-hungry appliances in buildings
93 increasingly contribute to global warming. To reduce energy consumption, a possible solution
94 may be found in the passive design of buildings. This entails using a complete set of chosen
95 materials in building construction as well as specific technical solutions [2] to reach high energy
96 efficiency, therefore rendering energy-hungry appliances useless. To achieve this aim, insulation
97 products are used to improve the building's behaviour. Indeed, insulation of the building
98 envelope makes it possible to retain heat during winter and decrease heat loads during summer.
99 Furthermore, thermal insulation can save energy and improve the comfort of the building
100 because heat flow is reduced.

101 Additional thermal insulation can be used to help improve the energy efficiency of a
102 building. With this objective in mind, phase change materials (PCMs) have been studied and
103 developed for certain applications [3]. These materials have higher thermal energy storage
104 densities than other heat storage materials. During a phase change process at constant
105 temperature, PCMs are able to store and release latent heat. Latent heat storage involves storing
106 energy during melting and energy release during freezing. Organic and inorganic PCMs are
107 often used and solid-liquid phases are chosen. Paraffin is the PCM most frequently used for
108 latent heat thermal energy storage. It has useful thermal properties such absence of super
109 cooling, chemical stability and low vapour pressure [4,5].

110 In this paper, the PCM chosen consists of 60% microencapsulated paraffin within a
111 copolymer and laminated with protective aluminium foil [6]. In addition to the phase change
112 process, the surface of the PCM acts as a reflective insulation. The action of reflective insulation
113 is usually closely linked to the radiative properties of the surface. The reflective surface reduces

114 the radiant heat transfer across an enclosed air space, for example between the metal and the
115 plasterboard in a specific roof configuration. According to reference [7], the air layer is used to
116 induce heat transfer by infrared radiation. The combination of homogenous and
117 inhomogeneous materials with the air layer can be qualified as a complex wall. A complex wall
118 can be defined as an assembly of materials separated by one or several air layers [7].
119 Nevertheless, such an assembly complicates the determination of thermal performance owing to
120 the multiple configurations of the air layer: opened or closed, naturally ventilated or ventilated
121 by force. Generally, studies on the thermal performance of a roof system do not take into
122 account the air layer [8]. It is important to characterize the thermal effects of a complex roof
123 incorporating PCM for the chosen configuration. Therefore, for the specific conditions of
124 Reunion Island (characterized by a tropical and humid climate with strong solar radiation),
125 experimental and numerical approaches were conducted. A methodology was set up to
126 determine both the thermal behaviour and thermal performance of a complex roof with PCM.
127 In this article, the experimental study is presented. To begin with, it is important to highlight
128 that the methodology presented can be used for all climates, not only tropical and humid.

129 **2. Research statement and methodology**

130 2.1. Introduction

131 Located in the Indian Ocean, Reunion Island is a French overseas department
132 characterized by a tropical and humid climate. Microclimates make it an ideal location for
133 experimental investigation. During the summer, temperatures are generally above 30°C, with
134 wind speed oscillating between 0 and 1.5 m.s⁻¹, and the mean relative humidity is usually above
135 80%. It should be made clear that sometimes Reunion Island is subject to powerful and
136 destructive cyclones [2].

137 In Reunion Island, depending on the building materials used, buildings have different
138 thermal performance. Mainly wood and concrete have been used in construction. Recently, a
139 new type of residential building has appeared using concrete and traditional construction
140 materials. The roof consists of a corrugated sheet and a false ceiling. The false ceiling is
141 generally plywood or plasterboard. However, thermal insulation used in the roofing are not
142 effective. Usually, the roofs are inclined at 20°. The problem with these types of roof is the large
143 heat gain due to the roof coverings. The roof is the part with highest energy losses (20% to
144 30%) [9]. Furthermore, radiative effects must not be disregarded.

145 Thermal regulations have been implemented in Reunion Island since 2009 with
146 PERENE [10] and since 1st May 2010 with RTAA DOM to avoid construction of buildings with
147 different thermal performance. Current regulations make insulation and other technical
148 solutions compulsory to minimise the energy consumption of buildings. This major step in
149 building design reduces the need for air conditioning or heating systems and the harmful
150 effects they have on the environment.

151 2.2. Research statement

152 PCM incorporated in a typical roof in Reunion Island will result in complex physical
153 phenomena. PCM is inserted into an enclosed air space between the corrugated iron and
154 plasterboard. Once installed, an air layer is present between the corrugated iron, the surface of
155 the PCM and the metal. All heat transfers are fully combined and coupled. In this way, heat
156 transfer by conduction, convection and radiation has to be taken into account on the PCM
157 surface. Between the plasterboard and the PCM, only heat transferred by conduction is
158 considered.

159 The ventilation of the air layer is an important parameter. The thermal performance of
160 the roof varies depending on whether the air layer is naturally ventilated or force-ventilated [2].

161 Insertion of the PCM into the roof posed two problems for the chosen assembly:

- 162 – Will the temperature of the PCM enable phase change?
- 163 – What is the thermal performance of a complex roof with PCM?

164 A methodology was established and presented in order to solve these problems.

165 2.3. Methodology

166 The methodology is based on both numerical and experimental studies. From a
167 numerical viewpoint, a building simulation code called ISOLAB was developed by Miranville
168 during his thesis and recently a mathematical model dedicated to phase change materials
169 presented in [11,12] was implemented based on the heat apparent capacity method. From an
170 experimental point of view, a specific experimental platform was set up. For more details, refer
171 to [9].

172 This article focuses on the determination of thermal performance of a complex roof with
173 PCM and the results of an experimental protocol for a full-scale outdoor PCM test-cell in
174 Reunion Island. Usually, the equivalent thermal resistance is determined in steady-state
175 conditions whereas the focus of this paper is the determination of equivalent thermal resistance
176 in dynamic conditions. To obtain more precise information for the determination of equivalent
177 thermal resistance in these conditions, an international standard mean method [13] has been
178 used, and is explained in the following paragraph.

179 2.3.1. *The mean method*

180 To evaluate the thermal resistance from dynamic field measurements, the mean method
181 is used. This method is applied to dynamic data series and can be summarized by the following
182 equation (1):

$$R = \frac{\sum_{i=1}^n (T_{se,i} - T_{si,i})}{\sum_{i=1}^n \varphi_i} \quad (1)$$

$$\text{With: } \begin{cases} R \text{ thermal resistance of the wal} \\ T_{si,i} \text{ interior surface temperatur} \\ T_{se,i} \text{ exterior surface temperatur} \\ \varphi \text{ heat flux through the wall} \end{cases}$$

183 This method requires many conditions to validate the results and respect conservation of
 184 energy over the entire study period. To validate the results, two criteria must be respected
 185 during the calculation in order to determine the thermal resistance in steady-state conditions
 186 [2]:

- 187 1. The percentage difference (ε_1) between resistance calculated from the entire data
 188 series and resistance calculated from the database minus one day must be less
 189 than 5%.
- 190 2. The percentage difference (ε_2) between resistance calculated from the first $\frac{2}{3}$ of
 191 the data series and resistance calculated from the last $\frac{2}{3}$ of the database must be
 192 less than 5%.

193 Miranville implemented the mean method in the building simulation ISOLAB during his
 194 post-doctoral degree (authorisation to supervise PhD students). The method used was a specific
 195 model able to determine the thermal performance of building materials. This module is very
 196 easy to use. It requires either a series of simulation results or measurements from experimental
 197 data. The following figure illustrates the procedure:

198 *Figure 1: Calculation of thermal resistance in ISOLAB*

199 In this case, the complex roof consists of both homogenous and inhomogeneous material
 200 with an air layer with different modes of heat transfer. The presence of an air layer can have an
 201 impact on the thermal performance depending on convection intensity. The air layer can be
 202 ventilated or not and will modify heat transfer. These different conditions are taken into

203 account by the module and ensures conservation of energy during the study period.
204 Furthermore, the ε_1 and ε_2 indicators are verified as illustrated in Figure 1.

205 For the final calculation on a whole database or a part of it, the following parameters are
206 taken into account:

- 207 – Positive heat flux conduction
- 208 – Day-time selection
- 209 – Night-time selection
- 210 – User-time selection

211 According to reference [2], these criteria allow for a pre-treatment of the database and
212 increase the possibilities of exploitation of the data series. This approach constitutes an
213 alternative option when the validity of the final results is not obtained.

214 In this part, a brief description of the mean method was presented. See [14] for more
215 details.

216 3. Experimental environment

217 3.1. The experimental platform

218 The experimental platform was set up in the South of Reunion at the University Institute of
219 Technology of Saint-Pierre (Reunion Island) at a low altitude (55 m). The total area of this
220 platform was approximately 600m². Réunion has a tropical climate with strong solar radiation
221 and humidity. These climatic conditions offer ideal conditions for an experimental study. This
222 location was chosen by many researchers from the PIMENT laboratory to observe the
223 phenomena relative to building physics [9].

224 *Figure 2: Experimental devices*

225 On the experimentation site, two experimental buildings were installed (see Figure 2), a
226 small-scale device (named ISOTEST) [7,15] and a normal-scale (or unit scale) building (named
227 LGI) [7,9] (see Figure 3). The ISOTEST building corresponds to the LGI building on a smaller
228 scale. The different test cells are oriented north in order to receive symmetrical solar radiation.
229 The test cells do not shade each other, and thermal interactions between the cells are negligible.

230 *Figure 3: LGI and ISOTEST test cells*

231 Two meteorological stations are installed near the experimental buildings, in order to collect
232 meteorological data. These allows the data obtained by each one to be compared [9].

233 3.2. LGI test cell design

234 In order to observe building physics phenomena, an LGI test cell was used in real weather
235 conditions. With dimensions of 3m (height) \times 3m (width) \times 3m (length), it is representative of
236 a typical room in a building encountered in Reunion Island. The modular structure of the roof
237 allowed several configurations to be studied. The roof was inclined at 20° to the horizontal and
238 was equipped with PCM. The suspended ceiling is made of plasterboard and PCM. The
239 components of the LGI test cell are given in Table 1 and Figure 4.

240 *Table 1: Arrangement of the LGI test cell [12]*

241 *Figure 4: Exploded view of the LGI test cell roof*

242 With the aim of obtaining extreme condition input from the roof, a dark colour was
243 chosen for the corrugated covering. In order to have different experimental conditions, a
244 mechanical ventilation and split-system air conditioner were set up. For the experimental
245 sequence, the blind windows and the windowpanes in the door were masked as shown in
246 Figure 5. The geometric details without PCM were provided by [7]. The LGI test cell was
247 chosen because it represents a typical lightweight construction with a low thermal inertia.

248 *Figure 5: Experimental conditions*

249

250 3.3. LGI test cell instrumentation

251 Sixty sensors were used in the study. These were located both in the enclosure and on the
252 roof of the LGI test cell. The enclosure walls were equipped with thermal sensors on their
253 surfaces. To highlight the effect of air stratification, the interior volume was measured at three
254 different heights from the floor. The ground is the part of the building where the boundary
255 conditions are very difficult to measure and to overcome this problem, thermocouples were
256 placed in the concrete floor. Experimental measures are used as boundary conditions without
257 taking into account the ground model. This way, it possible to avoid errors in the code
258 validation step. The thermocouples were checked before use and were placed in three different
259 positions:

- 260 – On the inside surface of walls for surface temperature measurements
- 261 – Inserted in an aluminium cylinder for air temperature measurements
- 262 – Put inside a black globe for radiant temperature measurements

263 All surfaces of the complex roof were also instrumented. Heat fluxmeters were installed on
264 the roof surfaces, PCM and plasterboard to determinate the heat flux through the complex roof
265 with PCM. In the air layer, radiant and air temperatures were also measured as described above.

266 To ensure the accuracy of the measured data, protocol dictates that each thermocouple be
267 calibrated on site and that factory sensors be checked. Margin of error from the thermocouples
268 is about $\pm 0.5^{\circ}\text{C}$. According to the manufacturer's data, the error margin of the heat fluxmeters
269 is approximately 5%. The temperature error margin from the entire data acquisition system is
270 estimated to be $\pm 1^{\circ}\text{C}$.

271 A data logger was installed in the LGI test cell to automatically collect the data from the
272 sensors every 15 minutes. All data were saved on a computer.

273 3.4. Description of PCM test

274 In this paper, the PCM tested is the commercial product from Dupont™ called Energain®.
275 It is a flexible sheet 5 mm thick, made of 60% microencapsulated paraffin wax within a
276 copolymer laminated on both sides by an aluminium sheet. The dimensions of the
277 Dupont™Energain® are 5.26 mm in thickness, 1000 mm in width and 1198 mm in length.
278 The composite PCM heat capacity was measured using a differential scanning calorimeter. The
279 heating and the cooling rate is 0.05 K.min⁻¹. The freezing and heating curves are given in [6].
280 The latent heat of melting and freezing are 71 kJ.kg⁻¹ and 72.4 kJ.kg⁻¹ respectively, and the phase
281 change temperatures are 23.4°C and 17.7°C respectively. According to reference [6], the
282 difference between the melting temperature and the freezing temperature characterizes the
283 hysteresis of the material, i.e the fact that the mixture is not a eutectic. In their work, the
284 hysteresis effect is highlighted but in this case it is ignored. From the values given by
285 Dupont™Energain®, the densities are 750 kg.m⁻³ in liquid phase and 850 kg.m⁻³ in solid phase.
286 Thermal conductivities were measured using the guarded hot-plate test method [16]. The value
287 varies between 0.18 Wm⁻¹K⁻¹ (liquid phase) to 0.22 Wm⁻¹K⁻¹ (solid phase). These parameters are
288 dealt with in detail in [6,17].

289 3.5. Climatic data and experimental sequences

290 The tests were carried out between August and October 2012. After studying the data from
291 different meteorological stations on the site, this period was chosen to ensure phase change and
292 regeneration of the PCM. During the experimental sequences, the most important physical
293 variables were measured every day. Variables measured included, solar radiation (global, direct
294 and diffuse, on a horizontal plane), ambient air, exterior relative humidity, wind speed and

295 direction. The data is measured every minute, and every 15 minutes an average value is
296 calculated and saved.

297 The data from 20th September to 24th September 2012 are given in Figure 6.

298 *Figure 6: The climatic conditions during the experimental period [12]*

299 4. Results

300 4.1. Introduction

301 The experimental platform is located at low altitude and near the coast, and is subject to
302 variable weather all year round. The difference between summer and winter for experimental
303 location usually depends on wind conditions. Winter was chosen for the experimental sequence
304 presented here because this season offered ideal conditions for this study. In Figure 6, during
305 the daytime, exterior air temperature varied between 16°C and 27°C, global solar radiation
306 reached 1000 W.m² and was unchanged through the study period. The exterior relative
307 humidity rate oscillated between 60% and 80%, the mean of wind speed was generally 4 m.s⁻¹
308 except on one day when it reached 6 m.s⁻¹ (corresponding to trade winds) (Figure 6(b)). Trade
309 winds occur in winter in Reunion Island. On days where trade winds are observed, the exterior
310 air temperature is relatively low.

311 In order to obtain accurate measurements from the complex roof components, sensors
312 were placed at three levels (top, middle and bottom) and fully instrumented as shown in Figure
313 7. To ensure good experimental data, the middle values of the complex roof were used.

314 *Figure 7: Instrumentation of the complex roof*

315 4.2. Experimental results

316 To begin with, the curves obtained during the experimental period are in agreement with
317 the physical phenomena observed because from the roof cover to the inside surface of the

318 plasterboard, the temperature decreased. The corrugated iron is the surface where the solar
319 radiation is highest and will have a tendency to heat more than other walls of the complex roof.
320 In Figure 8, the temperature of a corrugated iron reached 50°C. However, according to
321 reference [2], the temperatures of the corrugated iron are often superior to the value obtained.

322 *Figure 8: Surface temperature of each roof component*

323 The maximum temperature difference between the inside plasterboard surface and the
324 outside PCM surface can reach 5°C (see Figure 9). These results are very interesting because
325 without using other thermal insulation and with a low PCM thickness, the inside surface
326 temperature of the plasterboard is reduced. However, it is necessary to check that the PCM
327 temperature is on either side of the melting temperature in order to regenerate it. That's why a
328 heat fluxmeter was installed on each surface as shown in Figure 10.

329 *Figure 9: Difference between exterior surface PCM temperature and inside plasterboard surface temperature*

330 *Figure 10: Heat fluxmeter on PCM exterior*

331 This step is required to ensure that the physical phenomena can be observed. According
332 to Figure 11, phase change occurred. The phase change shows that PCM installed is working at
333 full efficiency and justifies the chosen assembly. Although the air layer is not ventilated, PCM
334 regenerates during the night. This last point is important because performance may be
335 enhanced by ventilating the upper air layer and ensuring phase change every day without using
336 additional appliances. A study on the ventilation rate of the upper air layer is required. Thermal
337 insulation can be installed on the exterior PCM surface to enhance thermal comfort and give a
338 higher energetic performance of the LGI test cell.

339 *Figure 11: Phase change on 21th September 2012 (day)*

340 During the daytime, the heat flux measured in outside PCM surface is higher than the
341 inside plasterboard surface. At night, the phenomena are reversed. A plausible explanation may
342 be that during the day the energy is stored and during the night the energy is released by the

343 PCM. The temperature curves are consistent with heat flux curves and show that PCM is able
344 to reduce heat transfer from the outside to inside of the test cell. PCM is effective for the given
345 configuration.

346 ISOLAB has already been validated by the IEA BESTEST protocol (International Energy
347 Agency for Building Energy Simulation Test) for the LGI test cell without PCM. To highlight
348 its impact on the inside air temperature of the test cell, a simulation without PCM was run in
349 order to compare results from experimental data. These results are illustrated in Figure 12.
350 Without PCM, the inside air temperature is higher than the test cell equipped with PCM.
351 During the daytime, a peak difference of temperature of 2.4°C is observed. Temperature rise is
352 also delayed as shown by the curves [12].

353 *Figure 12: Comparison of test cell air temperature with and without PCM [12]*

354 4.3. Determination of the R-value

355 Experimental data and the mean method were used to determine the R-value of the
356 complex roof. The upper air layer is obstructed and no ventilation takes place. In this case, the
357 curve between the two roof boundaries is shown in Figure 13. Evolution of temperatures in the
358 roof covering and inside plasterboard is similar with an average value of 2.15°C, a minimum
359 value of 7.87°C, and a maximum value of 26.10°C. The heat flux through the roof is also
360 periodic, with an average value of 0.69 W.m⁻¹, the minimum and maximum values being -1.69
361 W.m⁻¹ and 5.53 W.m⁻¹ respectively.

362 *Figure 13: Heat flux through the roof and temperature difference between corrugated iron exterior and plasterboard interior.*

363 The R-value was calculated by applying the calculation module implemented in ISOLAB
364 code and leads to the following values:

$$\left\{ \begin{array}{l} R = 0.60 \text{ m}^2 \cdot \text{K} \cdot \text{W}^{-1} \\ \varepsilon_1 = 0.80\% \\ \varepsilon_2 = 5.61\% \end{array} \right.$$

365 Under steady-state conditions a hypothesis is obtained, the R-value being calculated using
366 the sum of thermal resistance of each wall and taking into account the exchanges of convection
367 and radiation, and applying the Reunion Island thermal rules on the air layer. This gives a value
368 of $R=0.61 \text{ m}^2\cdot\text{K}\cdot\text{W}^{-1}$. The value is of the same order as the one determined by the calculation
369 module. It is noticed that the R-value is very small and that the result was expected. This result
370 can be explained by the thickness of the upper air layer and thermal insulators that have not
371 been added to the complex roof. In addition, the air layer was not ventilated and hence heat
372 exchanges by convection are smaller. It should also be noted that the R-value is similar to that
373 obtained by a radiant barrier used on the same test cell. However, the thermal resistance value
374 is significant and shows that PCM alone can not be considered as a thermal insulator but as
375 supplementary insulation. This is consistent with the literature.

376 5. Conclusion

377 This article deals with the first experimental study carried out in Reunion Island on a complex
378 roof with PCM in real conditions. The significance of this article results both from the choice
379 to install PCM and the determination of thermal performance via the R-value in dynamic
380 conditions.

381 It was necessary to test PCM without using a thermal insulator in order to determine its
382 performance. A PCM was set up in these conditions to highlight the phase change process and
383 to use the reflective properties of its surfaces. The PCM phase change occurred and is
384 guaranteed for the given configuration. It is very interesting because PCM can regenerate
385 without the help of appliances. This is a positive point in terms of both energy consumption
386 and environmental impact because no fossil fuel is used to generate energy, to power appliances

387 to facilitate phase change. Thus, its inclusion in the complex roof reduces heat transfer, in most
388 cases by infrared radiation.

389 This configuration clearly showed the phase change phenomena. Comparison with the roof
390 without PCM made it possible to highlight the exact phenomena. On either side of the melting
391 temperature, it is observed that energy is stored during daytime and released during at night,
392 implying a delayed energetic demand. By adding PCM, the temperature of test cell was reduced
393 by approximately 2°C. Following these observations, the R-value was calculated in order to
394 evaluate PCM performance.

395 The mean method was used to asses thermal performance of the LGI test cell equipped with
396 PCM. The principle of conservation of energy was respected and was applied to the ISOLAB
397 code. Experimental measurements in realistic conditions were used. The results give a low R-
398 value corresponding to the experimental conditions. Furthermore, the mean method is able to
399 determinate the thermal performance of any building envelopes with PCM, and this value can
400 be improved by adding a layer of thermal insulation. The value obtained is equivalent to the
401 thermal performance of the radiant barrier value determined for the same LGI test cell.
402 However, other scenarios must be take into account such as a naturally ventilated or
403 mechanically ventilated air layer in order to determinate the R-values for these conditions.
404 Many experimental studies need to be done.

405 These particular components of the complex roof were chosen to obtain numerical values. The
406 numerical code developed is able to take into account the thermal behaviour of building
407 envelopes, including PCM, and was incorporated into the ISOLAB code. The results of the
408 numerical simulation and validation of the thermal model will be presented in a future
409 publication.

410

411 Acknowledgment

412 The authors wish to thank *Fonds Social Européen* and *La Région Réunion* for their support and
413 their funding of the first author's thesis.

414 6. References

- 415 [1] Pérez-Lombard L, Ortiz J, Pout C. A review on buildings energy consumption information.
416 *Energy and Buildings* 2008;40:394–8.
- 417 [2] Miranville F, Fakra AH, Guichard S, Boyer H, Praene J-P, Bigot D. Evaluation of the
418 thermal resistance of a roof-mounted multi-reflective radiant barrier for tropical and humid
419 conditions: Experimental study from field measurements. *Energy and Buildings*
420 2012;48:79–90.
- 421 [3] Farid MM, Khudhair AM, Razack SAK, Al-Hallaj S. A review on phase change energy
422 storage: materials and applications. *Energy Conversion and Management* 2004;45:1597–
423 615.
- 424 [4] Sharma A, Tyagi VV, Chen CR, Buddhi D. Review on thermal energy storage with phase
425 change materials and applications. *Renewable and Sustainable Energy Reviews*
426 2009;13:318–45.
- 427 [5] Zalba B, Marin JM, Cabeza LF, Mehling H. Review on thermal energy storage with phase
428 change: materials, heat transfer analysis and applications. *Applied Thermal Engineering*
429 2003;23:251–83.
- 430 [6] Kuznik F, Virgone J. Experimental investigation of wallboard containing phase change
431 material: Data for validation of numerical modeling. *Energy and Buildings* 2009;41:561–
432 70.

- 433 [7] Miranville F. Contribution à l'Etude des Parois Complexes en Physique du Bâtiment:
434 Modélisation, Expérimentation et Validation Expérimentale de Complexes de Toitures
435 incluant des Produits Minces Réfléchissants en climat tropical humide. Université de la
436 Réunion, 2002.
- 437 [8] Pasupathy A, Athanasius L, Velraj R, Seeniraj RV. Experimental investigation and
438 numerical simulation analysis on the thermal performance of a building roof incorporating
439 phase change material (PCM) for thermal management. Applied Thermal Engineering
440 2008;28:556-65.
- 441 [9] Guichard S. Contribution à l'étude des parois complexes intégrant des matériaux à
442 changement de phase: Modélisation, Expérimentation et Evaluation de la performance
443 énergétique globale. La Réunion, 2013.
- 444 [10] Garde F, David M, Adelard L, Ottenwelter E. Elaboration of thermal standards for French
445 tropical islands: presentation of the PERENE project. Clima 2005, Lausanne, Switzerland:
446 2005.
- 447 [11] Guichard S, Miranville F, Boyer H, La Réunion F. A mathematical model of Phase Change
448 Materials (PCMs) used in buildings. Proceedings of the Third IASTED African Conference,
449 vol. 684, 2010, p. 223.
- 450 [12] Guichard S, Miranville F, Bigot D, Boyer H. A thermal model for phase change materials
451 in a building roof for a tropical and humid climate: Model description and elements of
452 validation. Energy and Buildings 2014;70:71-80.
- 453 [13] Norme ISO-9869. Isolation thermique - Elements de construction - Mesures in-situ de la
454 résistance thermique et de la transmittance thermique 1994.

- 455 [14] Miranville F. Modélisation multizone intégrée et expérimentation in-situ en Physique du
456 Bâtiment: Application aux parois complexes isolantes actives et passives et aux conditions
457 de confort. 2009.
- 458 [15] Bigot D, Miranville F, Fakra AH, Boyer H. A nodal thermal model for photovoltaic
459 systems: Impact on building temperature fields and elements of validation for tropical and
460 humid climatic conditions. *Energy and Buildings* 2009;41:1117-26.
- 461 [16] C177-04 A. Standard test method for steady state heat flux measurements and thermal
462 transmission properties by means of the Guarded-Hot-Plate apparatus, American Society for
463 Testing and Materials Philadelphia, PA; 2004.
- 464 [17] David D, Kuznik F, Roux JJ. Numerical study of the influence of the convective heat
465 transfer on the dynamical behaviour of a phase change material wall. *Applied Thermal*
466 *Engineering* 2011;31:3117-24.



1
2
3
4
5
6
7
8
9
10
11
12
13
14
15
16
17
18
19
20
21

Submission of manuscript to Energy and Buildings

Experimental investigation on a complex roof incorporating phase-change material.

Stéphane GUICHARD, Frédéric MIRANVILLE, Dimitri BIGOT, Bruno MALET-DAMOUR and Harry BOYER

Contents:

- *List of captions*

Corresponding author:

Stéphane GUICHARD

Research Institute in Innovation and Business Sciences (IRISE) Laboratory\CESI-CCIR\CRITTThe

CESI engineering school

Campus Pro - CCIR

65 rue du Père Lafosse - Boîte n°4

97410 Saint-Pierre

tél : 06 92 78 06 71

fax : 02 62 96 28 59

email : sguichard@cesi.fr



22
23
24
25
26
27
28
29
30
31
32
33
34
35
36
37
38
39

List of captions of figures

- Figure 1: Calculation of thermal resistance in ISOLAB
- Figure 2: Experimental devices
- Figure 3: LGI and ISOTEST test cells
- Figure 4: Exploded view of the LGI test cell roof
- Figure 5: Experimental conditions
- Figure 6: The climatic conditions during the experimental period [12]
- Figure 7: Instrumentation of the complex roof
- Figure 8: Surface temperature of each roof component
- Figure 9: Difference between exterior surface PCM temperature and inside plasterboard surface temperature
- Figure 10: Heat fluxmeter on PCM exterior
- Figure 11: Phase change on 21th September 2012 (day)
- Figure 12: Comparison of test cell air temperature with and without PCM [12]
- Figure 13: Heat flux through the roof and temperature difference between corrugated iron exterior and plasterboard interior.



3

4 Submission of manuscript to Energy and Buildings

5 Experimental investigation on a complex roof incorporating phase-

6 change material.

7

8 Stéphane GUICHARD, Frédéric MIRANVILLE, Dimitri BIGOT, Bruno MALET-DAMOUR and Harry BOYER

9 Contents:

- 10
- *List of figures*

11 Corresponding author:

12 **Stéphane GUICHARD**

13 Research Institute in Innovation and Business Sciences (IRISE) Laboratory-CCIR\CRITT

14 The CESI engineering school

15 Campus Pro - CCIR

16 65 rue du Père Lafosse - Boîte n°4

17 97410 Saint-Pierre

18 tél : 06 92 78 06 71

19 email : sguichard@cesi.fr

20



List of figures

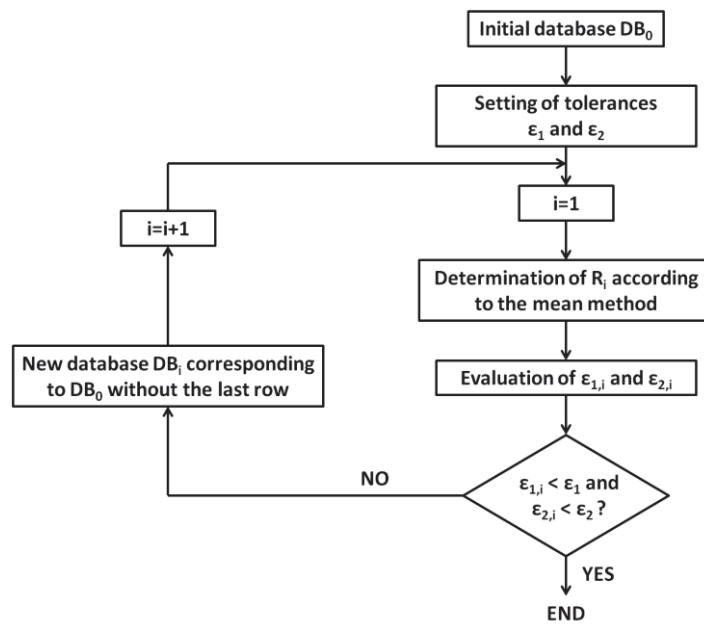


Figure 1: Calculation of thermal resistance in ISOLAB



Figure 2: Experimental devices



Figure 3: LGI and ISOTEST test cells

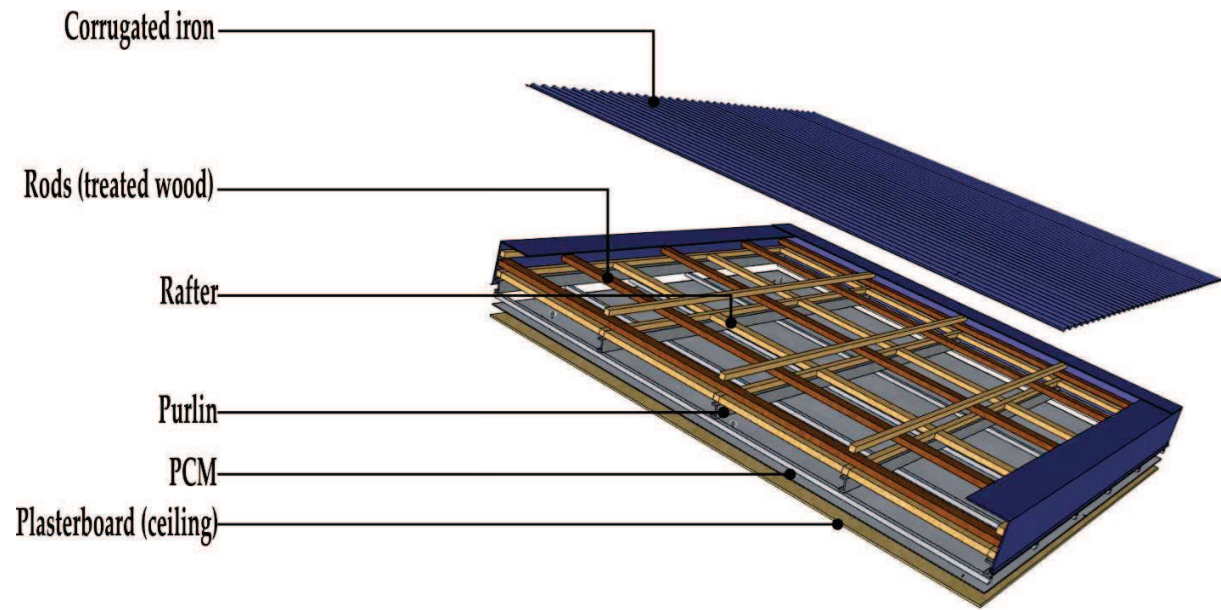


Figure 4: Exploded view of the LGI test cell roof

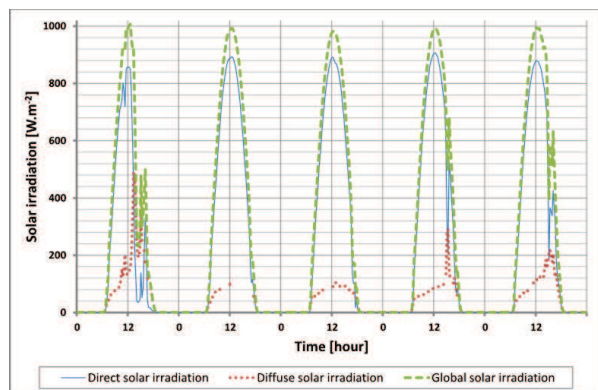


(a) Blind windows

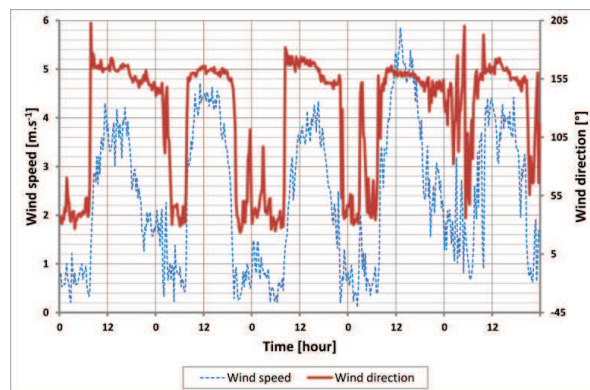


(b) The window panes in the door

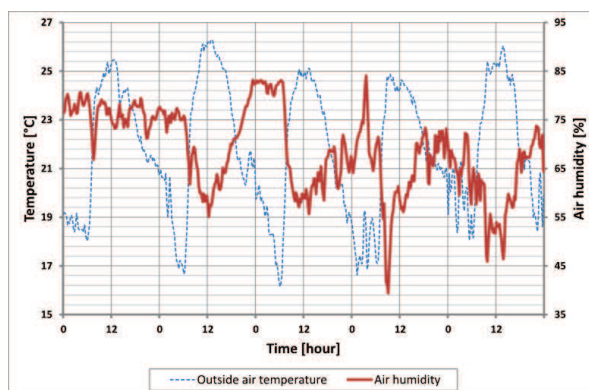
Figure 5: Experimental conditions



(a) Solar irradiation



(b) Wind speed and wind direction



(c) Outside air temperature and air humidity

Figure 6: The climatic conditions during the experimental period [12]

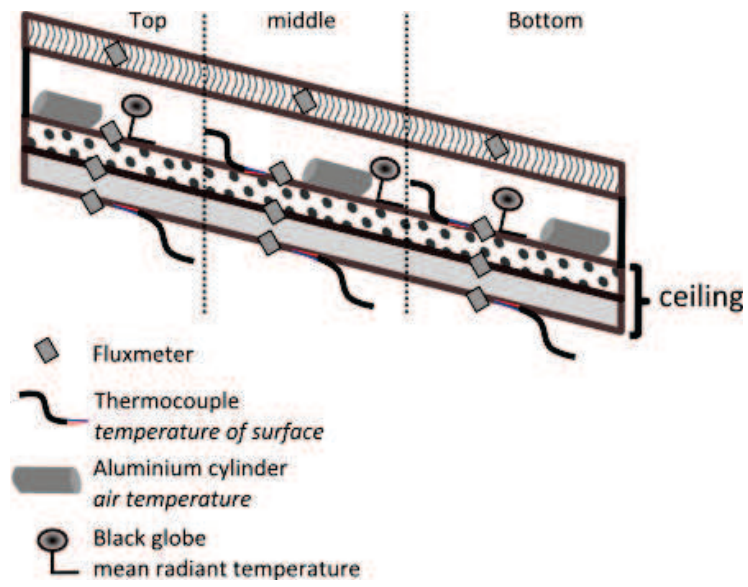
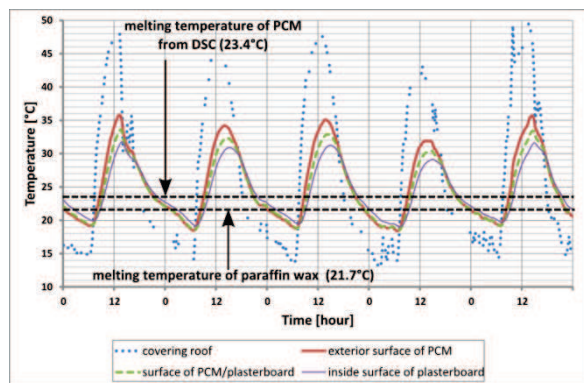
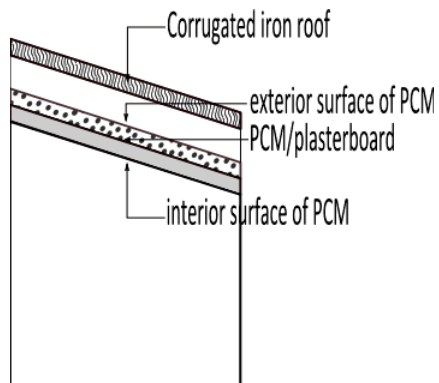


Figure 7: Instrumentation of the complex roof



(a) Temperature



(b) Localization

Figure 8: Surface temperature of each roof component

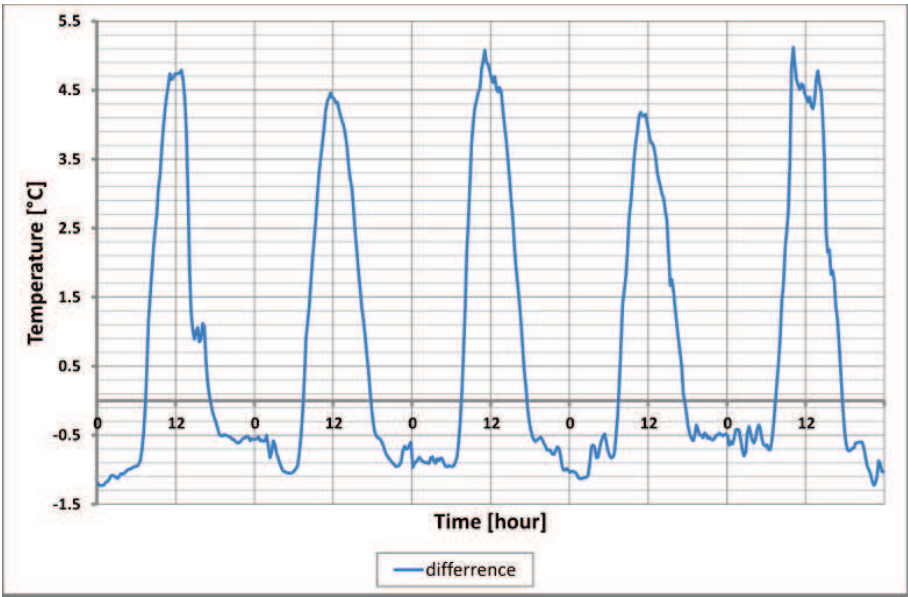


Figure 9: Difference between exterior surface PCM temperature and inside plasterboard surface temperature

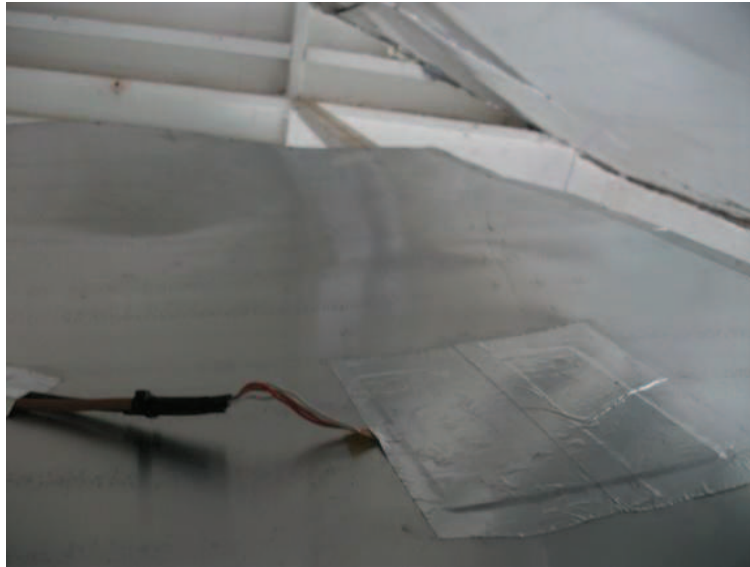


Figure 10: Heat fluxmeter on PCM exterior

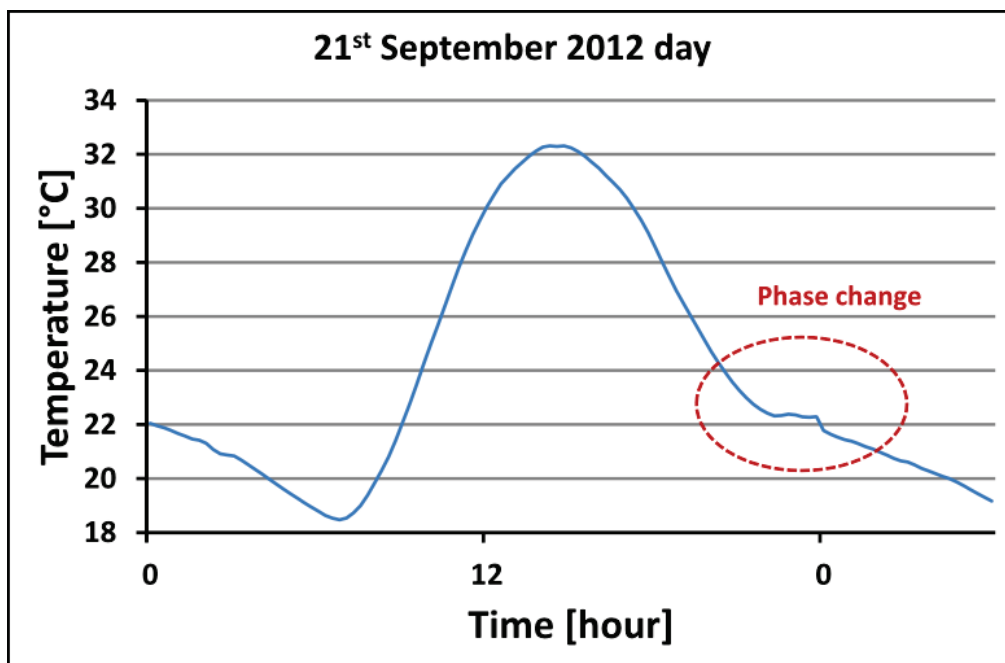


Figure 11: Phase change on 21th September 2012 (day)

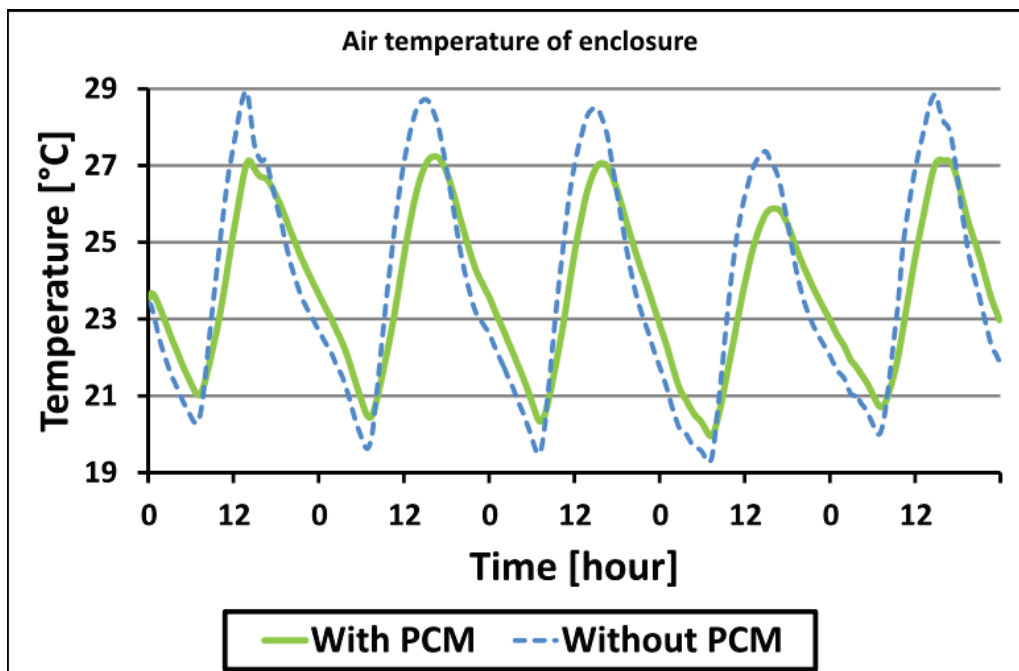
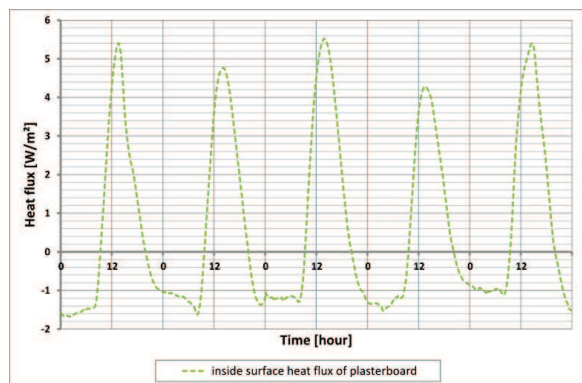
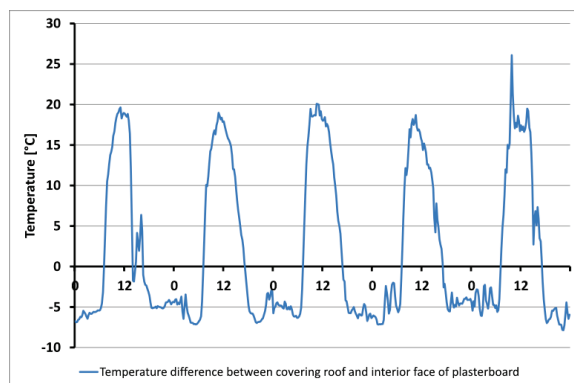


Figure 12: Comparison of test cell air temperature with and without PCM [12]



(a) Heat flux



(b) Temperature difference between the two boundaries of the roof

Figure 13: Heat flux through the roof and temperature difference between corrugated iron exterior and plasterboard interior.



3

4 Submission of manuscript to Energy and Buildings

5 Experimental investigation on a complex roof incorporating phase-
6 change material.

7

8 Stéphane GUICHARD, Frédéric MIRANVILLE, Dimitri BIGOT, Bruno MALET-DAMOUR and Harry BOYER

9 Contents:

- 10 • *List of tables*

11 Corresponding author:

12 **Stéphane GUICHARD**

13 Research Institute in Innovation and Business Sciences (IRISE) Laboratory-CCIR\CRITT

14 The CESI engineering school

15 Campus Pro - CCIR

16 65 rue du Père Lafosse - Boîte n°4

17 97410 Saint-Pierre

18 tél : 06 92 78 06 71

19 email : sguichard@cesi.fr



List of tables

<i>Element</i>	<i>Composition</i>	<i>Remark(s)</i>
Opaque vertical walls	Sandwich board 80mm thick cement-fiber / polyurethane / cement-fiber	
Window	Aluminium frame, 8 mm clear glass	Blind-type 0.8x0.8m
Glass door	Aluminium frame, 8mm clear glass	Glass in upper and lower parts, 0.7x2.2m
Roofing complex	Corrugated galvanised steel 1 mm/air layer of 280 mm thick/PCM 5.26 mm thick/ Plasterboard 12.5 mm	PCM is laminated to aluminium protective foils. Roof inclined at 20°
Floor	Concrete slabs 80mm thick on 60 mm thick polystyrene	

Table 1: Arrangement of the LGI test cell [12]



3

4

Submission of manuscript to Energy and Buildings

5 Experimental investigation on a complex roof incorporating phase-

6 change material.

7

8 Stéphane GUICHARD, Frédéric MIRANVILLE, Dimitri BIGOT, Bruno MALET-DAMOUR and Harry BOYER

9 Contents:

- 10
- *Highlights*

11

12 Corresponding author:

13 **Stéphane GUICHARD**

14 Research Institute in Innovation and Business Sciences (IRISE) Laboratory\CESI-CCIR\CRITT

15 The CESI engineering school

16 Campus Pro - CCIR

17 65 rue du Père Lafosse - Boîte n°4

18 97410 Saint-Pierre

19 tél : 06 92 78 06 71

20 email : sguichard@cesi.fr

21



22
23
24
25
26
27
28
29
30
31

Highlights

- First experimental investigation conducted in Reunion Island for a tropical and humid climate
- Experimental method to evaluate R-values of Phase Change Materials in a dynamic state
- The method used field measurements from an experimental test cell
- R-values are proposed for winter over a period of five days
- The mean method is used to determine thermal performance of Phase Change Materials